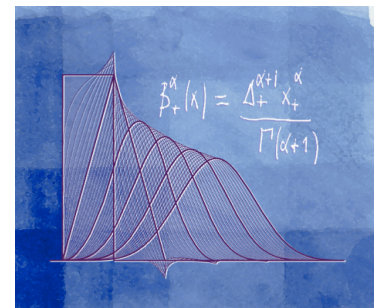


Wavelets, sparsity and biomedical image reconstruction

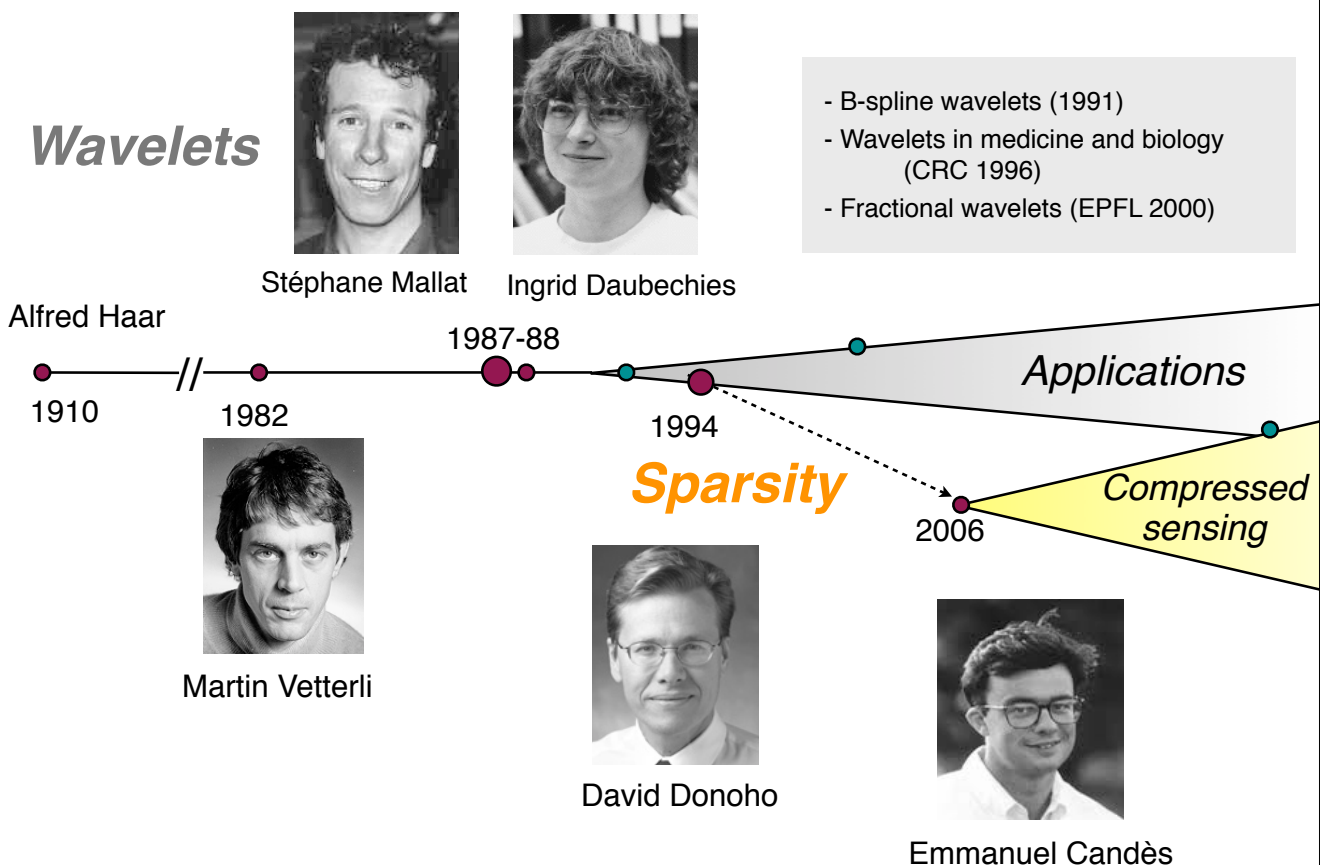
Michael Unser

Biomedical Imaging Group
EPFL, Lausanne, Switzerland



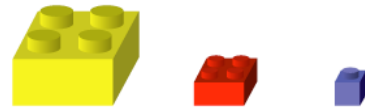
Imaging Seminar, University of Bern, Inselspital November 13, 2012

Brief history of wavelets



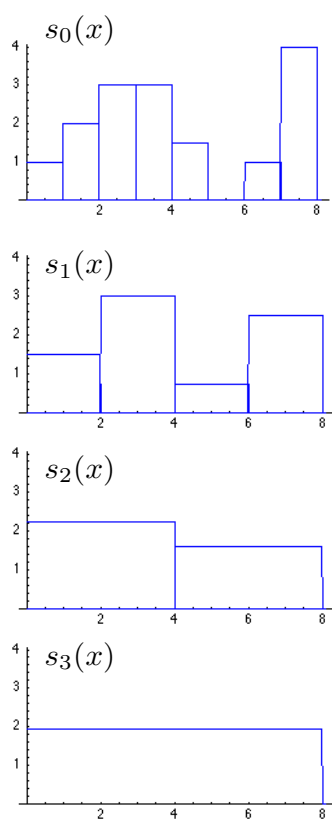
OUTLINE

- Short wavelet primer
 - From legos to wavelets
 - Sparsity
- Wavelet-domain image denoising
 - Soft-thresholding
 - SURELETS
- Image reconstruction with sparsity constraints
 - Compressed sensing
 - ISTA and faster variants
 - 3-D deconvolution microscopy
 - MRI



3

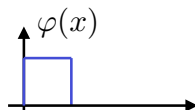
Wavelets: Haar transform revisited



Signal representation

$$s_0(x) = \sum_{k \in \mathbb{Z}} c[k] \varphi(x - k)$$

Scaling function



Multi-scale signal representation

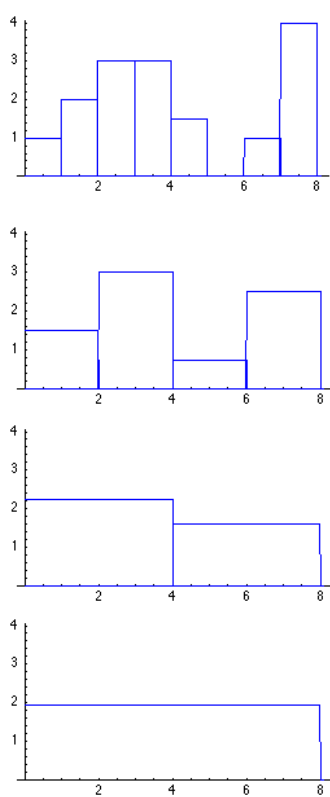
$$s_i(x) = \sum_{k \in \mathbb{Z}} c_i[k] \varphi_{i,k}(x)$$

Multi-scale basis functions

$$\varphi_{i,k}(x) = \varphi\left(\frac{x - 2^i k}{2^i}\right)$$

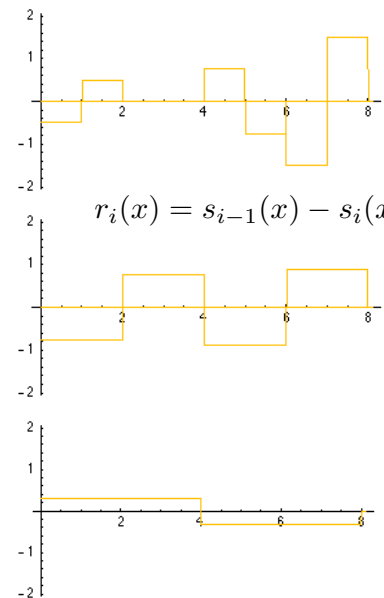
4

Wavelets: Haar transform revisited



Wavelet:

$$r_i(x) = s_{i-1}(x) - s_i(x)$$



5

Wavelets: Haar transform revisited

$$r_1(x) = \sum_k w_1[k] \psi_{1,k}$$

+

$$r_2(x) = \sum_k w_2[k] \psi_{2,k}$$

+

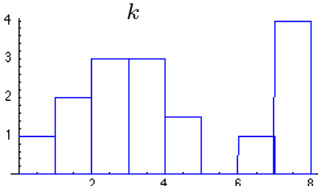
$$r_3(x) = \sum_k w_3[k] \psi_{3,k}$$

+

$$s_3(x) = \sum_k c_3[k] \varphi_{3,k}$$

Wavelet:

$$s(x) = \sum_k c[k] \varphi(x - k)$$



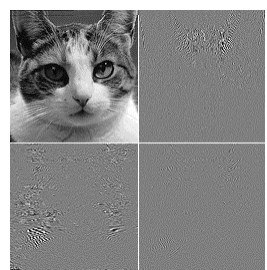
6

Haar wavelet and 2D basis functions



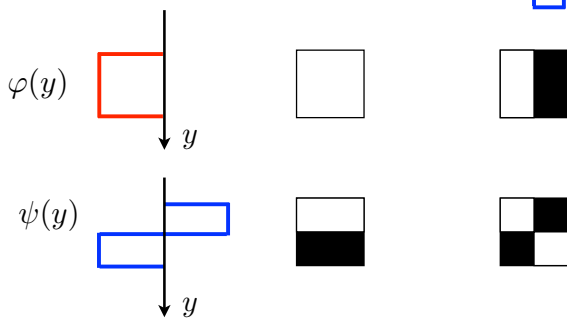
$$f(x, y) = \sum_{i, k} w_{i, k} \psi_{i, k}(x, y)$$

Expansion coefficients



Tensor-product basis functions

$$\begin{bmatrix} p_1 \\ p_2 \end{bmatrix} = \begin{bmatrix} \frac{1}{2} & \frac{1}{2} \\ \frac{1}{2} & -\frac{1}{2} \end{bmatrix} \cdot \begin{bmatrix} s \\ d \end{bmatrix}$$

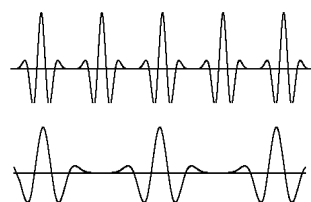


7

Sparsity of wavelet decomposition: example

Higher-order wavelets (splines)

$$f(x) = \sum_{i, k} \psi_{i, k}(x) w_{i, k}$$



Space-domain representation: $\mathbf{f} = \mathbf{Ww}$

Wavelet-domain representation: $\mathbf{w} = \mathbf{W}^{-1}\mathbf{f}$



66.4 dB

Wavelet transform

Inverse wavelet transform



0.00%

Discarding "small coefficients"

Reconstruction: $\mathbf{f}_N = \mathbf{Ww}_N$

Thresholding: $\mathbf{w} \rightarrow \mathbf{w}_N$

8

Wavelet transform as a mathematical microscope

Wavelet = Point Spread Function (PSF) of mathematical microscope

- Shape of PSF is the same at all scales
- Magnification by powers of two: 2^i
- Sampling is critical (no redundancy)
- Analysis functions (PSF) are orthogonal
- Resolution can be pushed to ultimate limit
⇒ existence of wavelet bases of $L_2(\mathbb{R})$

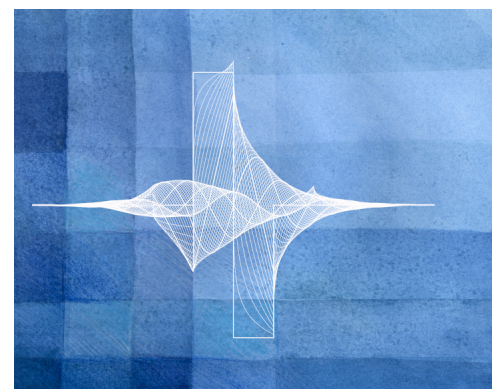
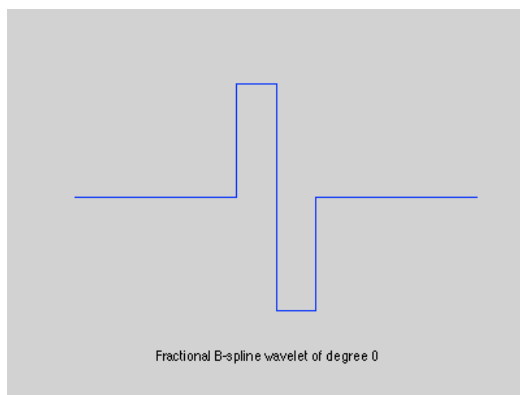


■ Desirable wavelet properties

short support, approximation order (vanishing moments) and differentiability

9

Beyond legos: Fractional B-spline wavelets



(Unser & Blu, *SIAM Rev*, 2000)

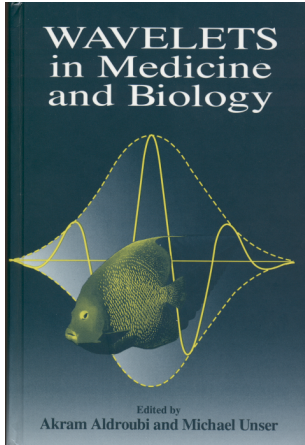
■ Remarkable property

Each of these wavelets generates a Riesz basis of $L_2(\mathbb{R})$

$$\psi_+^\alpha(x/2) = \sum_{k \in \mathbb{Z}} \frac{(-1)^k}{2^\alpha} \sum_{n \in \mathbb{N}} \binom{\alpha + 1}{n} \beta_*^{2\alpha+1}(n+k-1) \frac{\Delta_+^{\alpha+1}(x-k)_+^\alpha}{\Gamma(\alpha + 1)}$$

Only known wavelet bases that have an explicit time-domain formula !

10



Wavelets in medical imaging: Survey 1991-1999

References

- Unser and Aldroubi, *Proc IEEE*, 1996
- Laine, *Annual Rev Biomed Eng*, 2000
- Special issue, *IEEE Trans Med Im*, 2003

Image processing task	Application / modality	Principal Authors
Image compression	<ul style="list-style-type: none"> • MRI • Mammograms • CT • Angiograms, etc... 	Angelis 94; DeVore 95; Manduca 95; Wang 96; etc ...
Filtering	<i>Image enhancement</i>	Laine 94, 95;
	<ul style="list-style-type: none"> • Digital radiograms • MRI • Mammograms • Lung X-rays, CT 	Lu, 94; Qian 95; Guang 97; etc ...
	<i>Denoising</i>	Weaver 91; Xu 94; Coifman 95;
Feature extraction	<ul style="list-style-type: none"> • MRI • Ultrasound (speckle) • SPECT 	Abdel-Malek 97; Laine 98; Novak 98, 99
	<i>Detection of micro-calcifications</i>	Qian 95; Yoshida 94;
	<ul style="list-style-type: none"> • Mammograms 	Strickland 96; Dhawan 96; Bacayu 96; Heine 97; Wang 98
Texture analysis and classification	<i>Texture analysis and classification</i>	Barman 93; Laine 94; Unser 95; Wei 95; Yung 95; Busch 97; Mojsilovic 97
	<ul style="list-style-type: none"> • Ultrasound • CT, MRI • Mammograms 	
	<i>Snakes and active contours</i>	Chuang-Kuo 96
Wavelet encoding	<ul style="list-style-type: none"> • Ultrasound 	
	<ul style="list-style-type: none"> • Magnetic resonance imaging 	Weaver-Healy 92; Panych 94, 96; German 96; Shimizu 96; Jian 97
Image reconstruction	<i>Computer tomography</i>	Olson 93, 94; Peyrin 94;
	<ul style="list-style-type: none"> • Limited angle data • Optical tomography • PET, SPECT 	Walnut 93; Delaney 95; Sahiner 96; Zhu 97; Kolaczyk 94; Raheja 99
Statistical data analysis	<i>Functional imaging</i>	Ruttmann 93, 94, 98;
	<ul style="list-style-type: none"> • PET • fMRI 	Unser 95; Feilner 99; Raz 99
Multi-scale Registration	<i>Motion correction</i>	Unser 93; Thévenaz 95, 98;
	<ul style="list-style-type: none"> • fMRI, angiography • Multi-modality imaging • CT, PET, MRI 	Kybic 99
3D visualization	<ul style="list-style-type: none"> • CT, MRI 	Gross 95, 97; Muraki 95; Kamath 98; Horbelt 99

1

First published paper on biomedical applications

MAGNETIC RESONANCE IN MEDICINE 21, 288–295 (1991)

COMMUNICATIONS

Filtering Noise from Images with Wavelet Transforms

J. B. WEAVER,* YANSUN XU,* D. M. HEALY, JR.,† AND L. D. CROMWELL*

*Department of Radiology, Dartmouth-Hitchcock Medical Center; and †Department of Mathematics, Dartmouth College, Hanover, New Hampshire 03755

Received April 12, 1991

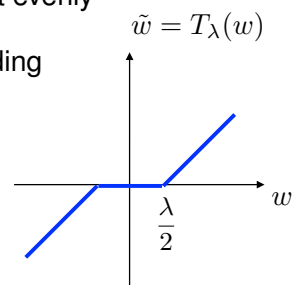
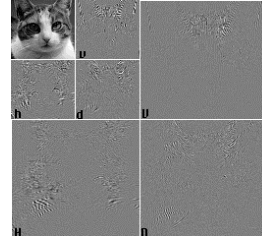
A new method of filtering MR images is presented that uses wavelet transforms instead of Fourier transforms. The new filtering method does not reduce the sharpness of edges. However, the new method does eliminate any small structures that are similar in size to the noise eliminated. There are many possible extensions of the filter. © 1991 Academic Press, Inc.

Denoising by wavelet thresholding

■ Basic idea

- Orthogonal WT: white noise \rightarrow white noise
- Signal is concentrated in few coefficients, while noise is spread-out evenly

\Rightarrow Noise attenuation is achieved by simple wavelet shrinkage/thresholding



■ References

- The pioneers
B. Weaver, X. Yansun, D.M. Healy Jr., and L.D. Cromwell, "Filtering noise from images with wavelet transforms," *Magnet. Reson. in Med.*, vol. 21, no. 2, pp. 288-295, 1991.
- Theoretical justification and link with sparsity
D.L. Donoho, "De-noising by soft-thresholding," *IEEE Trans. Information Theory*, vol. 41, no. 3, pp. 613-627, May 1995. (> 4000 ISI citations)

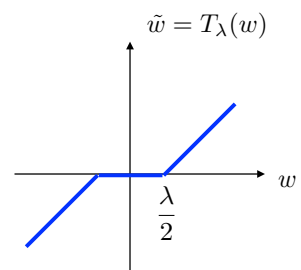
13

Wavelet denoising: variational interpretation

Signal + noise model : $\mathbf{y} = \mathbf{f} + \mathbf{n}$

■ Basic denoising algorithm

- Compute wavelet transform of noisy signal: $\mathbf{w} = \mathbf{W}^T \mathbf{y}$
- Apply pointwise non-linearity: $\tilde{\mathbf{w}} = T_\lambda\{\mathbf{w}\}$
- Compute inverse wavelet transform: $\tilde{\mathbf{f}} = \mathbf{W}\tilde{\mathbf{w}}$



■ Equivalent optimization problem

$$\tilde{\mathbf{w}} = \arg \min_{\mathbf{w}} \left\{ \|\mathbf{y} - \tilde{\mathbf{f}}\|_2^2 + \lambda \|\mathbf{w}\|_{\ell_1} \right\} \quad \text{with} \quad \tilde{\mathbf{f}} = \mathbf{W}\tilde{\mathbf{w}}$$

(LASSO Tibshirani *J. Royal Statist. Soc.* 1996; Chambolle et al., *IEEE Trans. Im Proc.* 1998)

14

BIG extension: SURE-LET

■ Key features of SURE-LET wavelet denoising algorithm

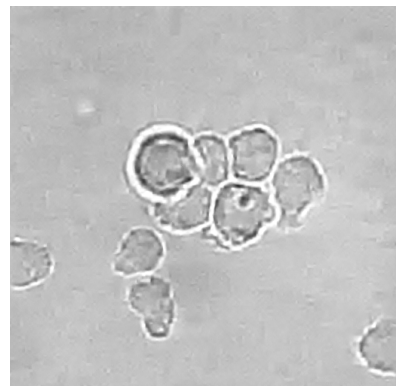
- Generalized non-linearities: Linear Expansion of Thresholds:

$$T_\lambda(w) \rightarrow \sum_{k=1}^K a_k f_k(w)$$

- Optimizes thresholding parameters a_k from noisy data using Stein's Unbiased Risk Estimate (SURE)
- Incorporates inter-scale dependencies via prediction tree
- Improved performance:
 - 1 to 1.5 dB better than basic soft thresholding
 - Very close to oracle performance
 - Outperforms standard Wiener filter

(Luisier et al., *IEEE Trans. Image Proc.* 2007)

SURE-LET Demo



SNR improvement: + 15.73 dB



2009 Young Author Best Paper Award
IEEE Signal Processing Society

15

Standard Color Image



Input PSNR=18.59 dB

16

Denoised with OWT SURE-LET



Output PSNR = 31.91 dB

17

Denoised with UWT SURE-LET



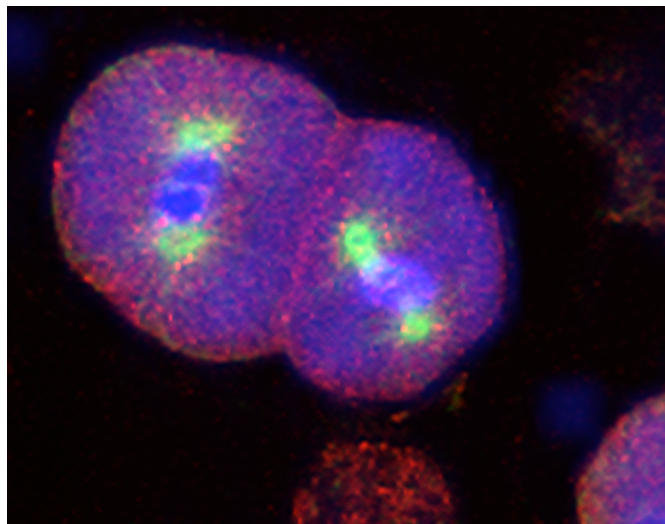
Output PSNR = 33.27 dB

18

PureDenoise (plugin for ImageJ)

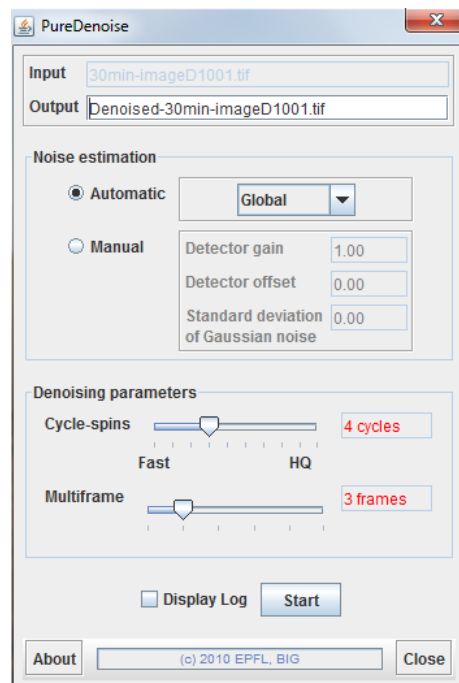
SURE-LET denoising

(Poisson + Gaussian noise, UWT)



C-elegance embryo

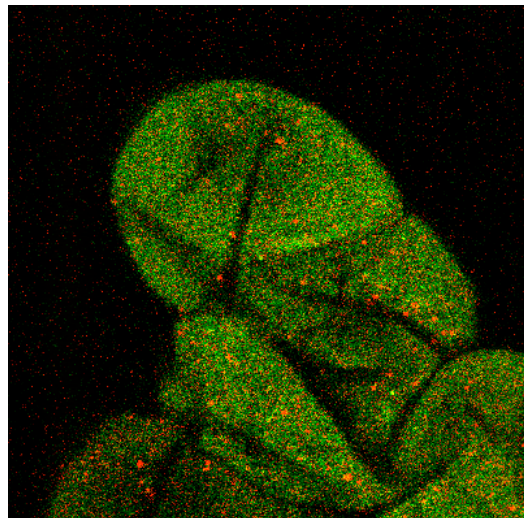
(Luisier et al., *Sig. Proc.* 2010)



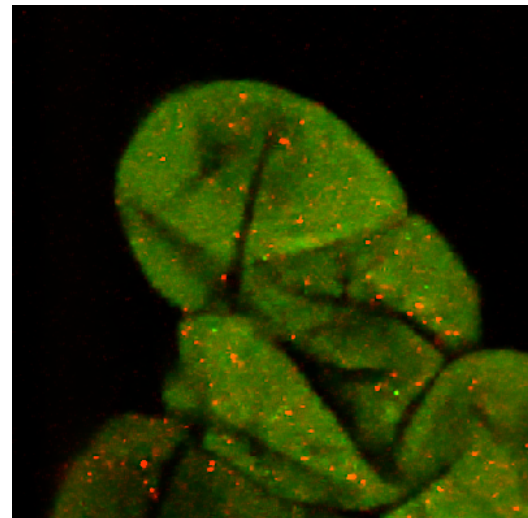
<http://bigwww.epfl.ch/algorithms/>

19

2D PureDenoise (UWT): Tobacco cells

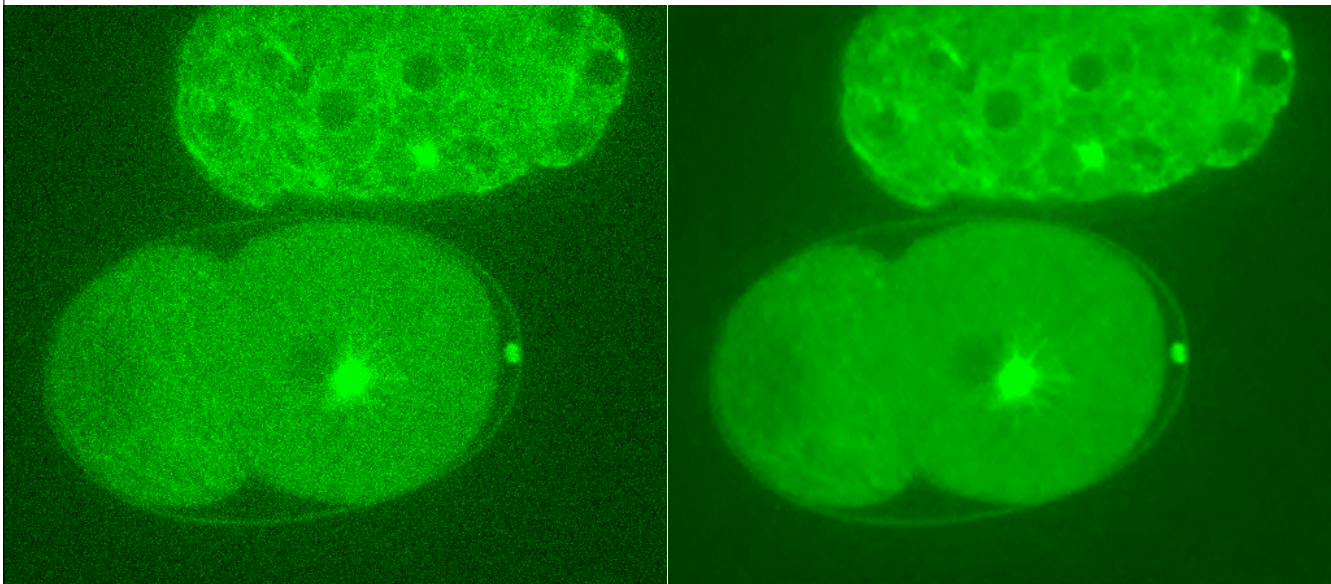


Ground truth
(average over 500 acquisitions)



20

2D + time SURE-LET denoising (DWT) : C-elegance embryo



21

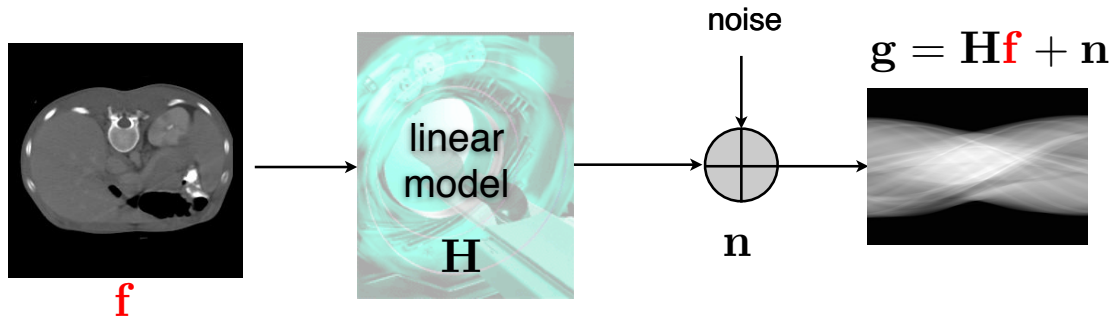
WAVELET-REGULARIZED IMAGE RECONSTRUCTION

- Imaging as an inverse problem
- Sparsity and wavelet regularization
 - Theory of compressed sensing
 - Sparsity and l_1 -minimization
- ISTA (Iterative Shrinkage-thresholding)
- Faster algorithms: ML-ISTA, FISTA, FWISTA
- Applications
 - 3-D deconvolution fluorescence microscopy
 - MRI reconstruction

22

Imaging as an inverse problem

■ Linear forward model



Ill-posed inverse problem: recover f from noisy measurements g

MRI: \mathbf{H} Fourier matrix (possibly, non-cartesian)

3-D fluorescence microscopy: \mathbf{H} (convolution matrix)

23

Theory of compressive sensing

■ Generalized sampling setting (after discretization)

- Linear inverse problem: $\mathbf{u} = \mathbf{H}\mathbf{f} + \mathbf{n}$
- Sparse representation of signal: $\mathbf{f} = \mathbf{W}\mathbf{v}$ with $\|\mathbf{v}\|_0 = K \ll N_v$
- $N_u \times N_v$ system matrix : $\mathbf{A} = \mathbf{H}\mathbf{W}$

■ Formulation of ill-posed recovery problem when $2K < N_u \ll N_v$

$$(P0) \quad \min_{\mathbf{v}} \|\mathbf{u} - \mathbf{A}\mathbf{v}\|_2^2 \quad \text{subject to} \quad \|\mathbf{v}\|_0 \leq K$$

■ Theoretical result

Under suitable conditions on \mathbf{A} (e.g., restricted isometry), the solution is unique and the recovery problem (P0) is equivalent to:

$$(P1) \quad \min_{\mathbf{v}} \|\mathbf{u} - \mathbf{A}\mathbf{v}\|_2^2 \quad \text{subject to} \quad \|\mathbf{v}\|_1 \leq C_1$$

[Donoho et al., 2005
Candès-Tao, 2006, ...]

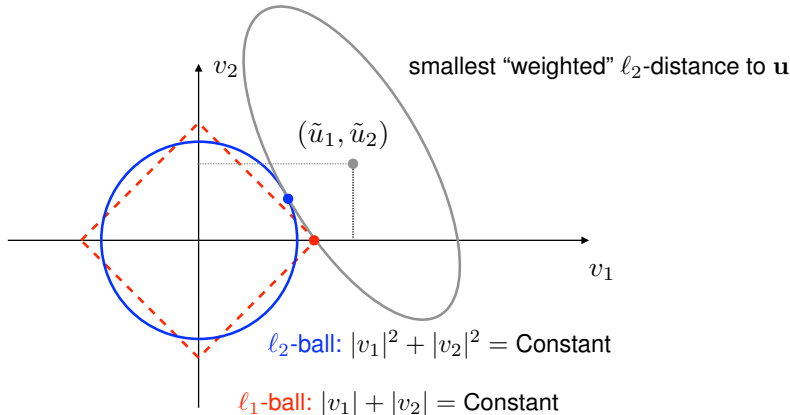
24

Sparsity and ℓ_1 -minimization

■ Prototypical inverse problem

$$\min_{\mathbf{v}} \left\{ \|\mathbf{u} - \mathbf{A}\mathbf{v}\|_{\ell_2}^2 + \lambda \|\mathbf{v}\|_{\ell_2}^2 \right\} \Leftrightarrow \min_{\mathbf{v}} \|\mathbf{u} - \mathbf{A}\mathbf{v}\|_{\ell_2}^2 \text{ subject to } \|\mathbf{v}\|_{\ell_2} = C_2$$

$$\min_{\mathbf{v}} \left\{ \|\mathbf{u} - \mathbf{A}\mathbf{v}\|_{\ell_2}^2 + \lambda \|\mathbf{v}\|_{\ell_1} \right\} \Leftrightarrow \min_{\mathbf{v}} \|\mathbf{u} - \mathbf{A}\mathbf{v}\|_{\ell_2}^2 \text{ subject to } \|\mathbf{v}\|_{\ell_1} = C_1$$

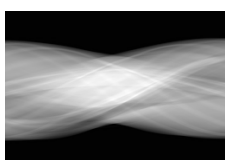


$$\text{Elliptical norm: } \|\mathbf{u} - \mathbf{A}\mathbf{v}\|_2^2 = (\mathbf{v} - \tilde{\mathbf{u}})^T \mathbf{A}^T \mathbf{A} (\mathbf{v} - \tilde{\mathbf{u}}) \quad \text{with} \quad \tilde{\mathbf{u}} = \mathbf{A}^{-1}\mathbf{u}$$

25

Wavelet-regularized image reconstruction

$$\mathbf{g} = \mathbf{H}\mathbf{f} + \mathbf{n}$$



Hypotheses:

- System matrix \mathbf{H} is known (physics)
- $\mathbf{f} = \mathbf{W}\mathbf{w}$ has a “sparse” wavelet expansion

■ Reconstruction as a (convex) optimization problem

$$\mathbf{f}^* = \operatorname{argmin}_{\mathbf{f}} \underbrace{\|\mathbf{g} - \mathbf{H}\mathbf{f}\|_2^2}_{\text{data consistency}} + \lambda \underbrace{\|\mathbf{W}^{-1}\mathbf{f}\|_{\ell_1}}_{\text{regularization}}$$

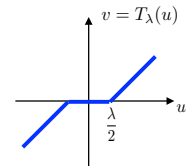
■ Iterative reconstruction algorithms

- | | |
|--|----------------------------------|
| ■ Generic ISTA (Iterative Soft-Thresholding Algorithm) | (Daubechies et al. 2004) |
| ■ 3-D deconvolution microscopy: ML-ISTA (Multi-level ISTA) | (C. Vonesch, Ph.D. thesis) |
| ■ MRI reconstruction: WFISTA (Weighted fast ISTA) | (M. Guerquin-Kern, Ph.D. thesis) |

26

Alternating minimization: ISTA

- Convex cost functional: $J(\mathbf{f}) = \|\mathbf{g} - \mathbf{H}\mathbf{f}\|_2^2 + \lambda\|\mathbf{W}^T\mathbf{f}\|_1$
- Special cases
 - Classical least squares: $\lambda = 0 \Rightarrow \mathbf{f} = (\mathbf{H}^T\mathbf{H})^{-1}\mathbf{H}^T\mathbf{g}$
 - Landweber algorithm: $\mathbf{f}_{n+1} = \mathbf{f}_n + \tau\mathbf{H}^T(\mathbf{g} - \mathbf{H}\mathbf{f}_n)$ (steepest descent)
 - Pure denoising: $\mathbf{H} = \mathbf{I} \Rightarrow \mathbf{f} = \mathbf{W} T_\lambda\{\mathbf{W}^T\mathbf{g}\}$ (Chambolle et al., IEEE-IP 1998)
- Iterative Shrinkage-Thresholding Algorithm (ISTA)
 1. Initialization ($n \leftarrow 0$), $\mathbf{f}_0 = \mathbf{g}$ (Figueiredo, Nowak, IEEE-IP 2003)
 2. Landweber update: $\mathbf{z} = \mathbf{f}_n + \tau\mathbf{H}^T(\mathbf{g} - \mathbf{H}\mathbf{f}_n)$
 3. Wavelet denoising: $\mathbf{w} = \mathbf{W}^T\mathbf{z}$, $\tilde{\mathbf{w}} = T_{\tau\lambda}\{\mathbf{w}\}$ (soft threshold)
 4. Signal update: $\mathbf{f}_{n+1} \leftarrow \mathbf{W}\tilde{\mathbf{w}}$ and repeat from Step 2 until convergence



Proof of convergence: (Daubechies, Defrise, De Mol, 2004)

27

Extension: General proximity operators

- Moreau's proximity operator with strength $\lambda > 0$

$$\text{prox}_\Phi(\mathbf{u}; \lambda) = \arg \min_{\mathbf{v} \in \mathbb{R}^N} \frac{1}{2} \|\mathbf{u} - \mathbf{v}\|^2 + \lambda \Phi(\mathbf{v})$$

Lower semicontinuous, convex function $\Phi : \mathbb{R}^N \mapsto \mathbb{R}$

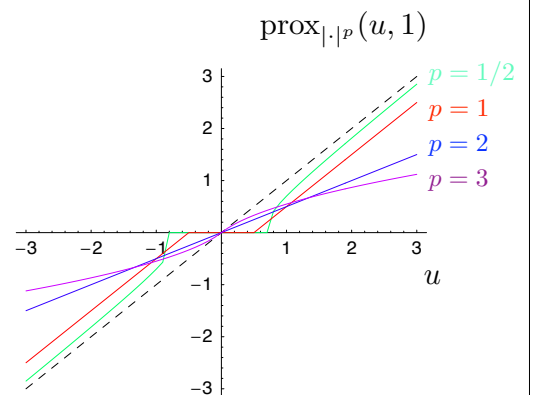
[Combettes-Pesquet, SIAM, 2007]

- Scalar proximity operator = non-linear map

$$\text{prox}_\Phi(u; \lambda) = \arg \min_v \frac{1}{2} \|u - v\|^2 + \lambda \Phi(v)$$

Potential function $\Phi(v)$

- Symmetric: $\Phi(v) = \Phi(-v)$
- Non-decreasing, but not necessarily convex
- Examples: $\Phi(v) = \lambda|v|^p$ with $0 \leq p \leq \infty$



28

Extended ISTA: Iterative Shrinkage/thresholding

$$\text{Minimize: } J(\mathbf{v}) = \frac{1}{2} \|\mathbf{u} - \mathbf{Av}\|_2^2 + \lambda \sum_n \Phi(v_n) \quad \Rightarrow \quad \mathbf{v}^* = \arg \min_{\mathbf{v}} J(\mathbf{v})$$

- Extended ISTA algorithm: wavelet-domain formulation

```

input:  $\mathbf{A}, \mathbf{u}, \mathbf{v}_0, \lambda \in \mathbb{R}^+$ 
Initialization:  $n = 0$ 
Repeat
     $\mathbf{v}_{n+1} = \text{prox}_{\Phi}(\mathbf{v}_n + \tau \mathbf{A}^T (\mathbf{u} - \mathbf{A}\mathbf{v}_n); \lambda\tau)$ 
     $n \leftarrow n + 1$ 
until Stopping criterion
return  $\mathbf{v}_n$ 

```

$\Phi : \mathbb{R} \mapsto \mathbb{R}$ (lower semicontinuous, convex)

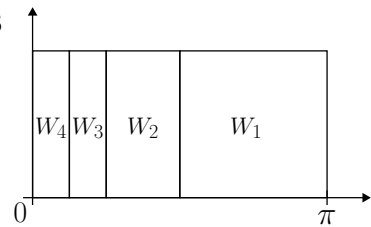
$$\text{Convergence guarantee: } J(\mathbf{v}_n) - J(\mathbf{v}^*) \leq \frac{L}{n} \|\mathbf{v}_0 - \mathbf{v}^*\|_2^2$$

29

Faster scheme: deconvolution in a Shannon basis

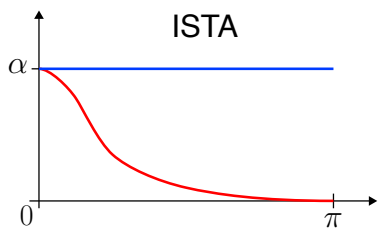
- Characteristics of Shannon's wavelet basis

- Orthonormality
- Wavelet subspaces correspond to ideal frequency subbands

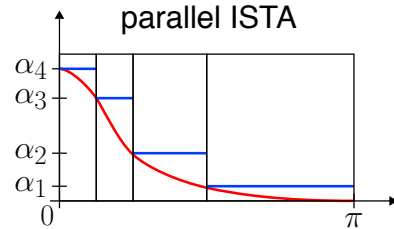


- \mathbf{H} circulant \Rightarrow decoupled optimization across subbands

$$\|\mathbf{HWw}\|_2^2 = \sum_{j \in S} \|\mathbf{HW}_j \mathbf{w}_j\|_2^2 \leq \sum_{j \in S} \alpha_j \|\mathbf{W}_j \mathbf{w}_j\|_2^2 = \sum_{j \in S} \alpha_j \|\mathbf{w}_j\|_2^2$$



\Rightarrow Substantial acceleration of ISTA



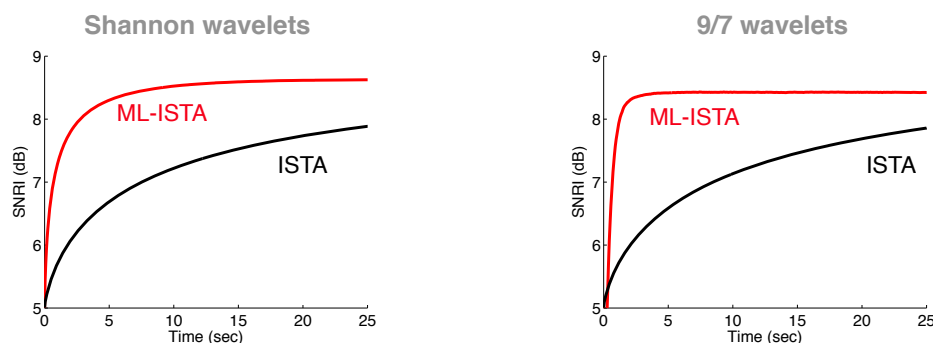
(Vonesch-U., IEEE-IP, 2008)

30

Fast multilevel wavelet-regularized deconvolution

■ Key features of multilevel wavelet deconvolution algorithm (ML-ISTA)

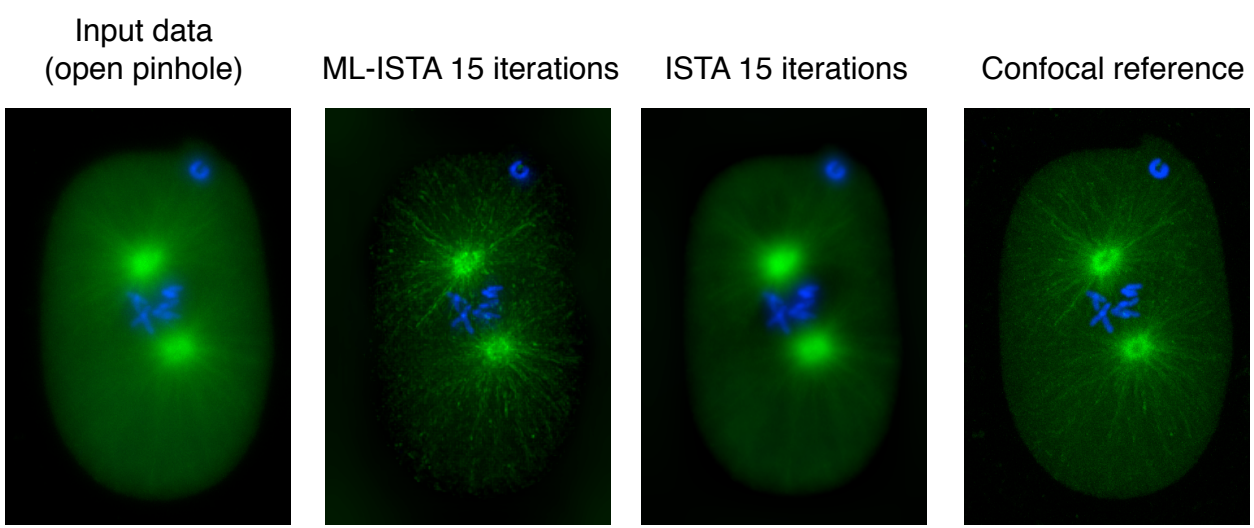
- Acceleration by one order of magnitude with respect to ISTA (multigrid iteration strategy)
- Applicable in 2D or 3D:
first wavelet attempt for the deconvolution of 3D fluorescence micrographs
- Works for any wavelet basis
- Typically outperforms oracle Wiener solution (best linear algorithm)



(Vonesch-Unser, *IEEE-IP*, 2009)

31

Wavelet-regularized 3-D deconvolution microscopy

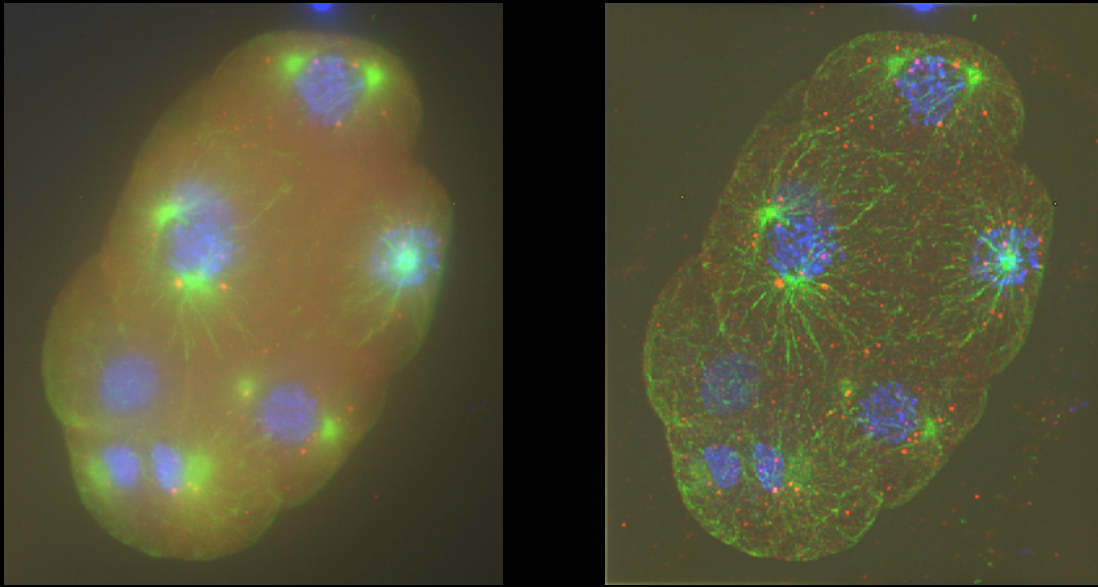


(Vonesch-U. *IEEE Trans. Im. Proc.* 2009)

Maximum-intensity projections of $512 \times 352 \times 96$ image stacks;
Zeiss LSM 510 confocal microscope with a $63\times$ oil-immersion objective;
C. Elegans embryo labeled with Hoechst, Alexa488, Alexa568;
each channel processed separately; computed PSF based on diffraction-limited model;
separable orthonormalized linear-spline/Haar basis.

32

3D deconvolution of widefield stack



Maximum intensity projections of $384 \times 448 \times 260$ image stacks;
 Leica DM 5500 widefield epifluorescence microscope with a $63 \times$ oil-immersion objective;
 C. elegans embryo labeled with Hoechst, Alexa488, Alexa568;
 each channel processed separately; computed PSF based on diffraction-limited model;
 Haar basis, 3 decomposition levels for X-Y, 2 decomposition levels for Z.

FISTA: Fast ISTA

Wavelet expansion: $\mathbf{f} = \mathbf{W}\mathbf{w}$

Global system matrix: $\mathbf{A} = \mathbf{H}\mathbf{W}$

- ISTA: repetition of a simple fixed-point operation

$$\mathbf{w}_{n+1} = \mathcal{P}(\mathbf{w}_n)$$

- Guaranteed convergence

[Daubechies et al, 2004]

$$\lim_{n \rightarrow \infty} \mathbf{w}_n = \mathbf{w}^* \quad \text{with} \quad \mathbf{f}^* = \mathbf{W}\mathbf{w}^*$$

... but slow

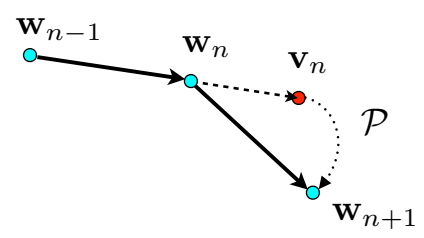
[Beck and Teboulle, 2009]

$$J(\mathbf{w}_n) - J(\mathbf{w}^*) = \mathcal{O}(1/n)$$

- FISTA= controlled over-relaxation

[Beck & Teboulle, 2009]

$$J(\mathbf{w}_n) - J(\mathbf{w}^*) = \mathcal{O}(1/n^2)$$



FISTA: Fast ISTA

[Beck and Teboulle, 2009]

Minimize: $J(\mathbf{v}) = \frac{1}{2} \|\mathbf{u} - \mathbf{Av}\|_2^2 + \lambda \|\mathbf{v}\|_1$

Solution: $\mathbf{v}^* = \arg \min_{\mathbf{v}} J(\mathbf{v})$

- FISTA algorithm: wavelet-domain formulation

```

input:  $\mathbf{A}, \mathbf{u}, \mathbf{v}_0, \lambda \in \mathbb{R}^+$ 
Initialization:  $n = 0, t_0 = 1, \mathbf{w}_0 = \mathbf{0}$ 
Repeat
 $\mathbf{w}_{n+1} = \text{prox}(\mathbf{v}_n + \tau \mathbf{A}^T (\mathbf{u} - \mathbf{Av}_n); \lambda \tau)$ 
 $t_{n+1} = \frac{1 + \sqrt{1 + 4t_n^2}}{2}$ 
 $\mathbf{v}_{n+1} = \mathbf{w}_{n+1} + \left( \frac{t_n - 1}{t_{n+1}} \right) (\mathbf{w}_{n+1} - \mathbf{w}_n)$ 
 $n \leftarrow n + 1$ 
until Stopping criterion
return  $\mathbf{v}_n$ 

```

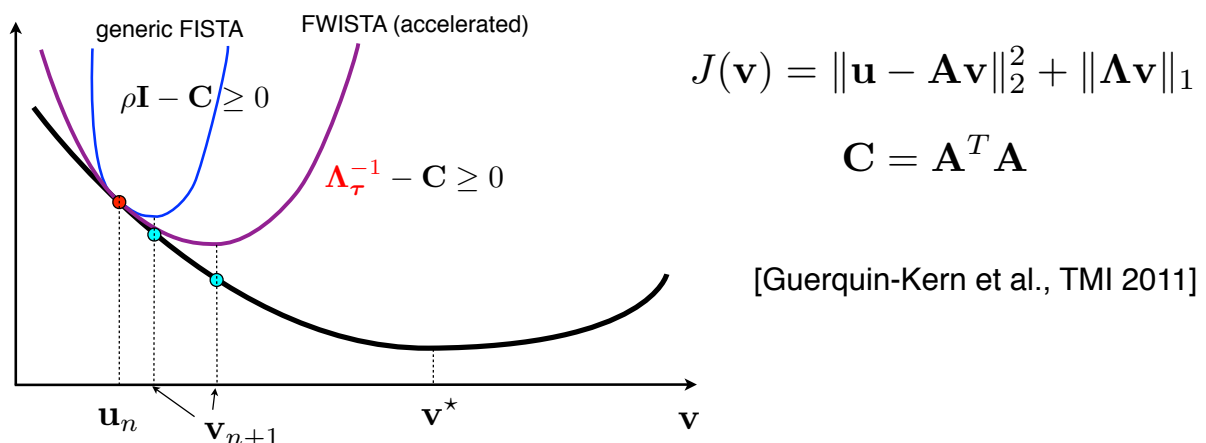
Convergence guarantee: $J(\mathbf{v}_n) - J(\mathbf{v}^*) \leq \frac{4L}{(n+1)^2} \|\mathbf{v}_0 - \mathbf{v}^*\|_2^2$

35

FWISTA: Fast weighted ISTA

Idea: **Adaptive** step size/regularization tailored to the problem

$$\rho(\mathbf{C}) \rightarrow \Lambda_\tau^{-1} \quad \text{or/and} \quad \lambda \rightarrow \Lambda$$



Sharper quadratic upper bound

\Rightarrow faster convergence at same computational cost

36

FWISTA: Fast weighted ISTA

Minimize: $J(\mathbf{v}) = \frac{1}{2} \|\mathbf{u} - \mathbf{Av}\|_2^2 + \lambda \|\mathbf{v}\|_1$

Solution: $\mathbf{v}^* = \arg \min_{\mathbf{v}} J(\mathbf{v})$

- FWISTA algorithm: wavelet-domain formulation

input: $\mathbf{C} = \mathbf{A}^T \mathbf{A}$, $\mathbf{c} = \mathbf{A}^T \mathbf{u}$, \mathbf{v}_0 , $\Lambda = \text{diag}(\boldsymbol{\tau})$

Initialization: $n = 0$, $t_0 = 1$

Repeat

$$\mathbf{w}_{n+1} = \text{prox}(\mathbf{v}_n + \Lambda(\mathbf{c} - \mathbf{C}\mathbf{v}_n); \lambda\boldsymbol{\tau})$$

$$t_{n+1} = \frac{1 + \sqrt{1 + 4t_n^2}}{2}$$

$$\mathbf{v}_{n+1} = \mathbf{w}_{n+1} + \left(\frac{t_n - 1}{t_{n+1}} \right) (\mathbf{w}_{n+1} - \mathbf{w}_n)$$

$$n \leftarrow n + 1$$

until Stopping criterion

return \mathbf{v}_n

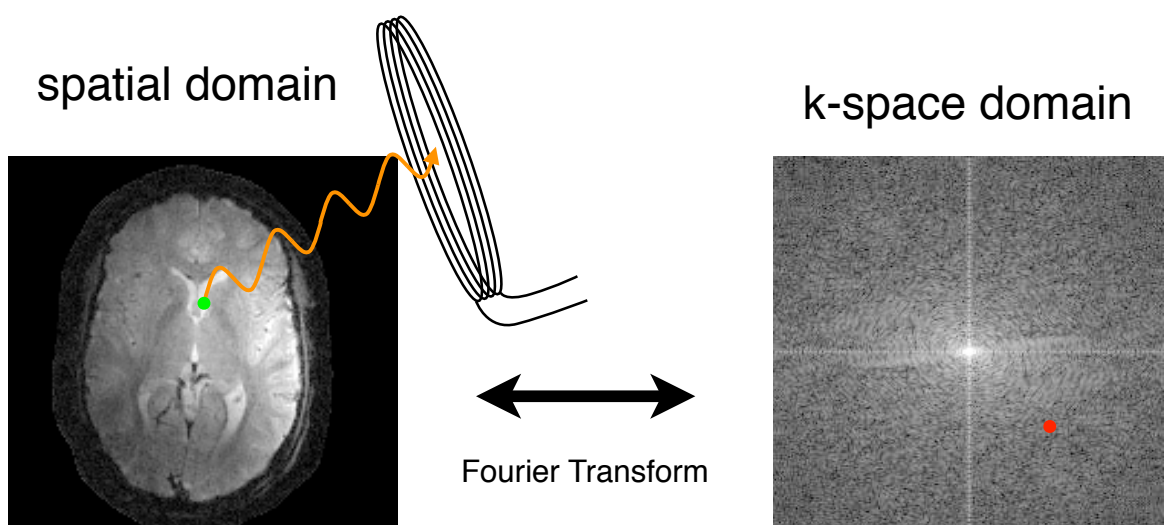
Condition for convergence:
 $(\Lambda^{-1} - \mathbf{C})$ positive definite

better constant

Convergence guarantee: $J(\mathbf{v}_n) - J(\mathbf{v}^*) \leq \frac{4}{(n+1)^2} \|\Lambda^{-1/2}(\mathbf{v}_0 - \mathbf{v}^*)\|_2^2$

37

Application: Parallel MRI reconstruction



$$S(\mathbf{r})f(\mathbf{r})$$

$$g(\mathbf{k}) = \int S(\mathbf{r})f(\mathbf{r})e^{j\langle \mathbf{r}, \mathbf{k} \rangle} d\mathbf{r}$$

Parallel MRI: several receiving coils, known sensitivities

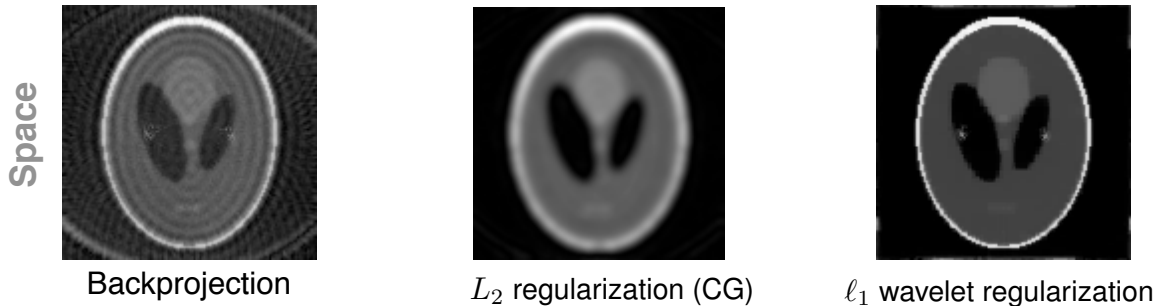
Challenging reconstruction: few k-space samples

38

Simulated parallel MRI experiment

Shepp-Logan brain phantom

4 coils, undersampled spiral acquisition, 15dB noise



[Guerquin-Kern et al., TMI 2011]

NCCBI collaboration with K. Prüssmann, ETHZ

39

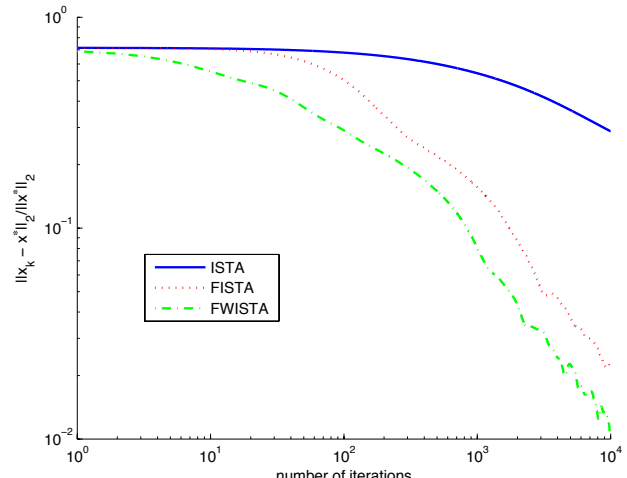
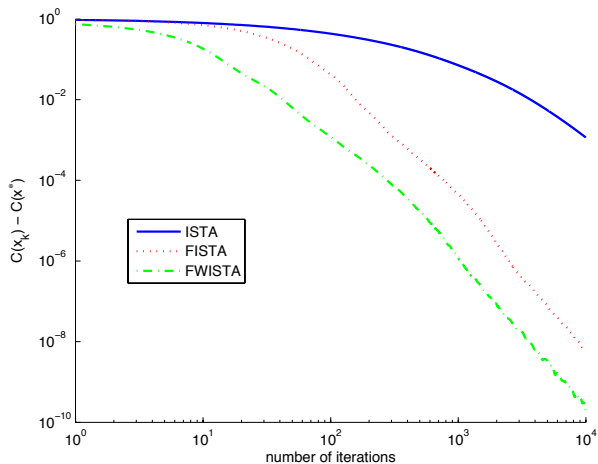
MRI: convergence results

Simulation parameters

- 176 radial trajectory
- 90 interleaves
- 4 receiving coils
- 40 dB of noise

Wavelet-based reconstruction

- 2-level Haar wavelet transform



MRI: reconstructions

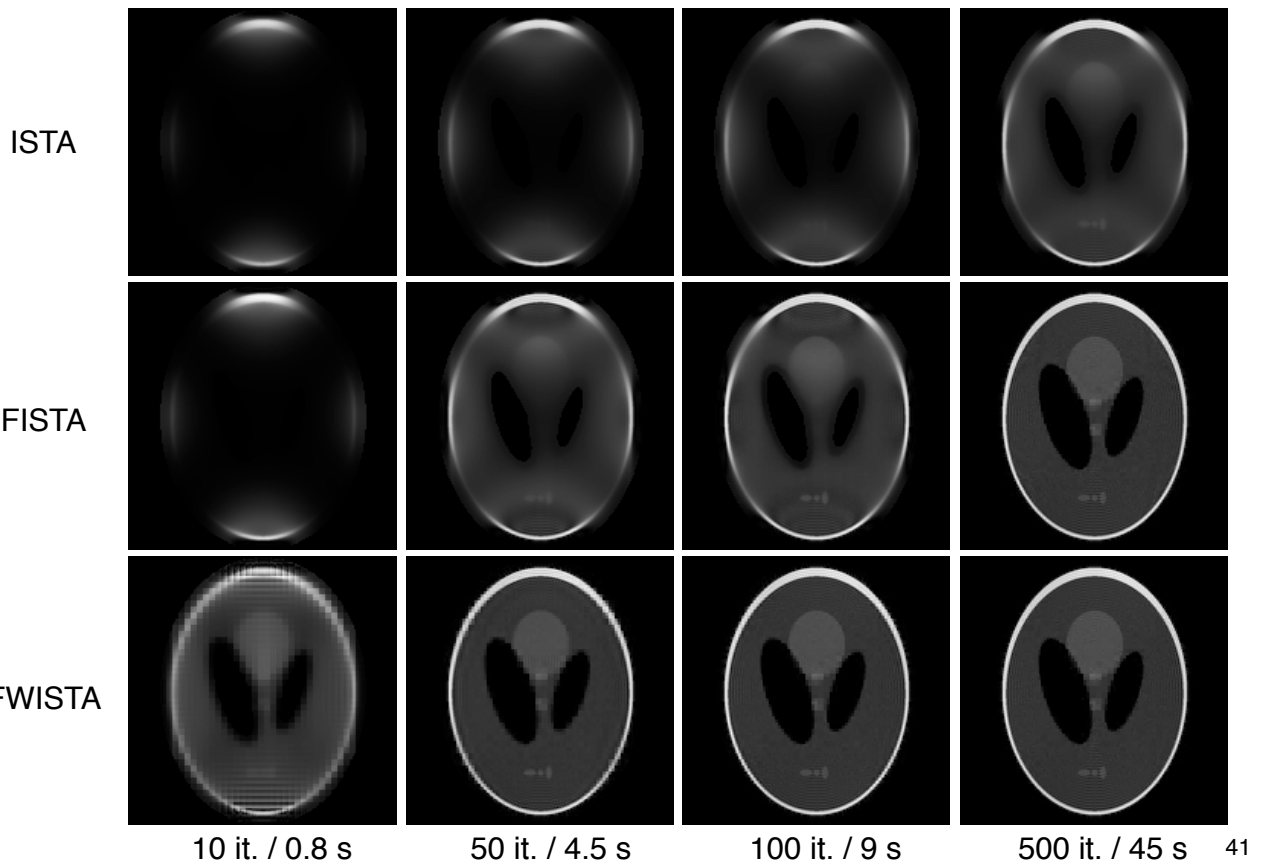


Fig. 1. Reference images from left to right: *in vivo* brain, SL reference, and wrist.

TABLE II
VALUES OF THE OPTIMAL SER AND CORRESPONDING REGULARIZATION PARAMETERS ARE SHOWN FOR THE DIFFERENT WAVELET BASES

Experiment		SL simulation				Wrist simulation			
Wavelet basis		Haar	Spline 2	Spline 4	Spline 6	Haar	Spline 2	Spline 4	Spline 6
Without RS	SER (dB)	12.65	12.16	10.75	9.70	15.93	17.33	17.32	17.07
	λ	1870	2510	830	1460	1600	946	1070	1350
With RS	SER (dB)	13.38	12.53	11.58	10.38	18.70	18.24	18.05	17.87
	λ	5650	3900	7770	1370	1490	850	1190	1260

TABLE IV
RESULTS OF THE ALGORITHMS CG (LINEAR), IRLS (TV), AND OUR METHOD (WAVELETS) FOR DIFFERENT DEPTHS. VALUES OF THE REGULARIZATION PARAMETER, THE FINAL SER, THE RELATIVE MAXIMAL SPATIAL DOMAIN ERROR, AND THE TIME TO REACH -0.5 dB OF THE FINAL SER

Experiment	SL simulation			Wrist simulation			Brain data		
	linear	TV	wavelets	linear	TV	wavelets	linear	TV	wavelets
λ opt.	0.0247	4.090	6.380	0.436	760	1.620	0.471	6.050	16.800
SER (dB) opt.	8.46	13.82	13.17	16.14	18.41	18.64	15.81	18.88	18.93
ℓ_∞ error (%)	48	49	51	21	16	16	29	12	11
$t_{-0.5\text{dB}}$ (s)	0.286	18.1	5.40	0.209	10.5	4.64	0.205	15.2	6.13

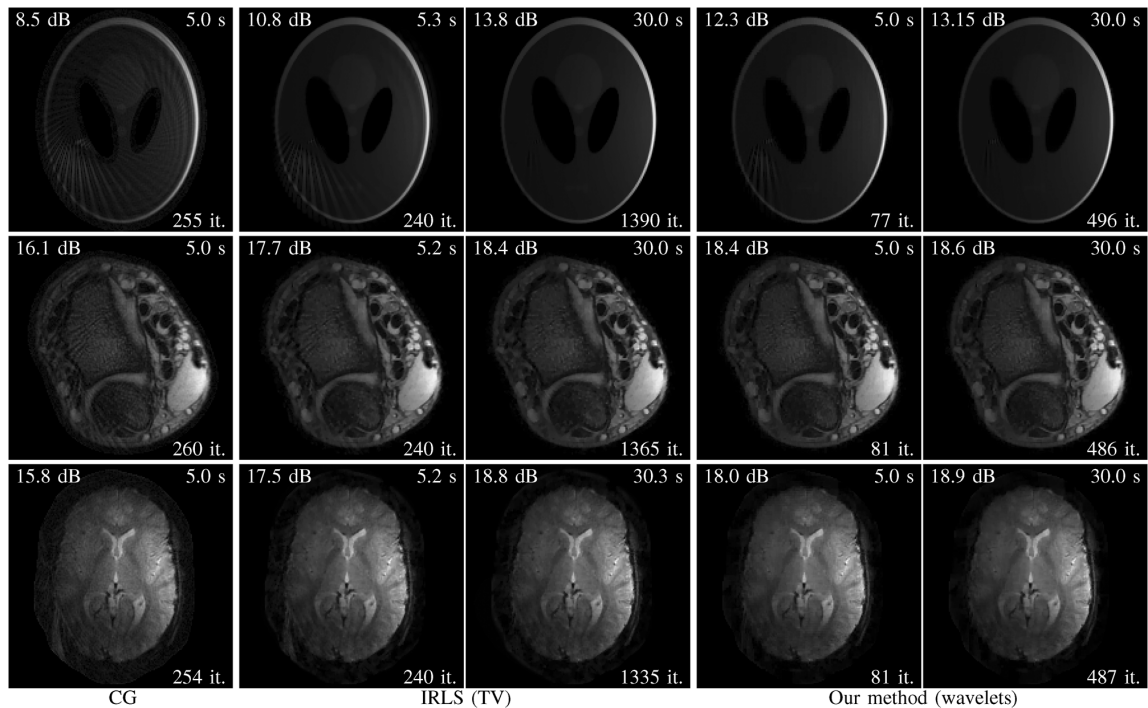


Fig. 5. Result of different reconstruction algorithms for the three experiments. For each reconstruction, the performance in SER with respect to the reference (top-left), the reconstruction time (top-right), and the number of iterations (bottom-right) are shown.

43

Wavelet-regularized reconstruction of MRI

L_2 regularization (Laplacian)



Standard approach (CG)

ℓ_1 wavelet regularization



WFISTA algorithm

(Guerquin-Kern et al. *IEEE Trans. Med. Im.* 2011)

44

CONCLUSION

- Important wavelet features
 - Simple, fast implementation: Mallat's filterbank algorithm
 - Mathematical properties: Riesz basis, vanishing moments,...
 - Simulates the organization of the primary visual system
- Many successful applications
 - Data compression
 - Filtering, denoising
 - Detection and feature extraction
 - Inverse problems: wavelet regularization
- Current topics in wavelet research and “compressed sensing”
 - Better wavelet dictionaries (frames): steerable wavelets, ...
 - Better (model-based) regularization schemes
 - Automatic parameter adjustment (e.g., scale-dependent threshold)
 - Addressing harder inverse problems

45

Acknowledgments



■ Biomedical Imaging Group

Senior scientists & Post docs

- Philippe Thévenaz, Ph.D.
- Daniel Sage, Ph.D.
- **Cédric Vonesch**, Ph.D.
- **Stamatis Lefkimiatis**, Ph.D.
- ...

Ph.D. Students

- Masih Nilchian, Ulugbek Kamilov, ...



Alumni

- Dr. François Aguet (Harvard)
- **Prof. Thierry Blu** (Chinese Univ., Hong Kong)
- Dr. Nicolas Chenouard (NYU)
- Prof. Mathews Jacob (Univ. Iowa)
- **Prof. Matthieu Querquin-Kern** (ENSEA)
- Prof. Michael Liebling (UC Santa Barbara)
- **Dr. Florian Luisier** (Harvard)
- Prof. D. Van De Ville (EPFL)
-

■ Swiss collaborations (NCCBI)

- **Prof Klaas Pruesmann, ETHZ**
- Prof. Marco Stampanoni, PSI/ETHZ

■ EPFL collaborators

- Dr. Arne Seitz
- Prof. Sebastian Maerkli
- Prof. John McKinney
- Prof. Ralf Gruetter
- Prof. Patrick Aebischer
-



46

Bibliography

■ Wavelet denoising and restoration

- A. Chambolle, R.A. DeVore, N.-Y. Lee and B.J. Lucier, "Nonlinear Wavelet Image Processing: Variational Problems, Compression, and Noise Removal Through Wavelet Shrinkage," *IEEE Trans. Image Processing*, vol. 7, no. 33, pp. 319-335, April 1998.
- F. Luisier, T. Blu, M. Unser, "A New SURE Approach to Image Denoising: Interscale Orthonormal Wavelet Thresholding," *IEEE Trans. Image Processing*, vol. 16, no. 3, pp. 593-606, March 2007.
- I. Daubechies, M. Defrise, and C. De Mol, "An Iterative Thresholding Algorithm for Linear Inverse Problems with a Sparsity Constraint," *Comm. Pure and Applied Mathematics*, vol. 57, no. 11, pp. 1413–1457, August 2004.
- A. Beck and M. Teboulle, "A fast iterative shrinkage-thresholding algorithm for linear inverse problems," *SIAM J. Imag. Sci.*, vol. 2, no. 1, pp. 183–202, 2009.
- C. Vonesch, M. Unser, "A Fast Multilevel Algorithm for Wavelet-Regularized Image Restoration," *IEEE Trans. Image Processing*, , vol. 18, no. 3, pp. 509-523, 2009.
- M. Guerquin-Kern, M. Häberlin, K.P. Pruessmann, M. Unser, "A Fast Wavelet-Based Reconstruction Method for Magnetic Resonance Imaging," *IEEE Trans. Medical Imaging*, vol. 30, no. 9, pp. 1649-1660, September 2011.

■ Review and tutorial

- M. Unser, A. Aldroubi, "A Review of Wavelets in Biomedical Applications," *Proc. of the IEEE*, vol. 84, no. 4, pp. 626-638, April 1996.
- M. Unser, T. Blu, "Wavelet Theory Demystified," *IEEE Trans. Sig. Proc.*, vol. 51, no. 2, pp. 470-483, 2003.
- M. Unser, M. Unser, "Wavelet Games," *Wavelet Digest*, vol. 11, no. 4, April 1, 2003.

Lego connection at: <http://www.wavelet.org/phpBB2/viewtopic.php?t=5129>